

## SEARCH FOR NEW PARTICLES AT LEP\*

ANDRÉ SOPCZAK

Karlsruhe University, D-76128 Karlsruhe, Germany

*(Received October 29, 1999)*

The latest preliminary results of the searches for Higgs bosons and Supersymmetric particles at LEP are reviewed. The results include the data-taking in 1999 up to center-of-mass energies of 196 GeV. The combination of the results from the four LEP experiments leads to a significant increase of the detection sensitivity. No indication of a signal has been observed. In the Standard Model (SM) a lower limit of 102.6 GeV on the mass of the Higgs boson is set at 95% CL. In extended models, stringent limits are also set on the  $HZZ$  coupling. Interpretations in the Minimal extension of the Supersymmetric Standard Model (MSSM) are given and the importance of general MSSM parameter scans is emphasized. In general scans, the limit on the mass of the lightest scalar Higgs boson is about 7 GeV lower in comparison with benchmark results. The data also constrains charged Higgs bosons of a general two-doublet model and Supersymmetric partners of the SM particles.

PACS numbers: 13.10.+q, 14.80.-j, 13.65.+i

**1. Introduction**

The data-taking at LEP has been very successful, leading to continuously increasing center-of-mass energy and luminosity as shown in Fig. 1. In August 1999, exactly 10 years after the first recording of a  $Z$  boson at LEP, a center-of-mass energy of 200 GeV was reached. The LEP accelerator will continue operation at a center-of-mass energy around 205 GeV in 2000.

The results of this report are mainly based on the combination of the data from the four LEP experiments ALEPH, DELPHI, L3 and OPAL [1]. In the search for the Standard Model Higgs boson, all four LEP experiments have contributed. Three experiments have released their 1999 data for combination in the MSSM search, and two for the charged Higgs boson search, as detailed in Table I.

---

\* Presented at the XXIII International School of Theoretical Physics "Recent Developments in Theory of Fundamental Interactions", Ustroń, Poland, September 15–22, 1999.

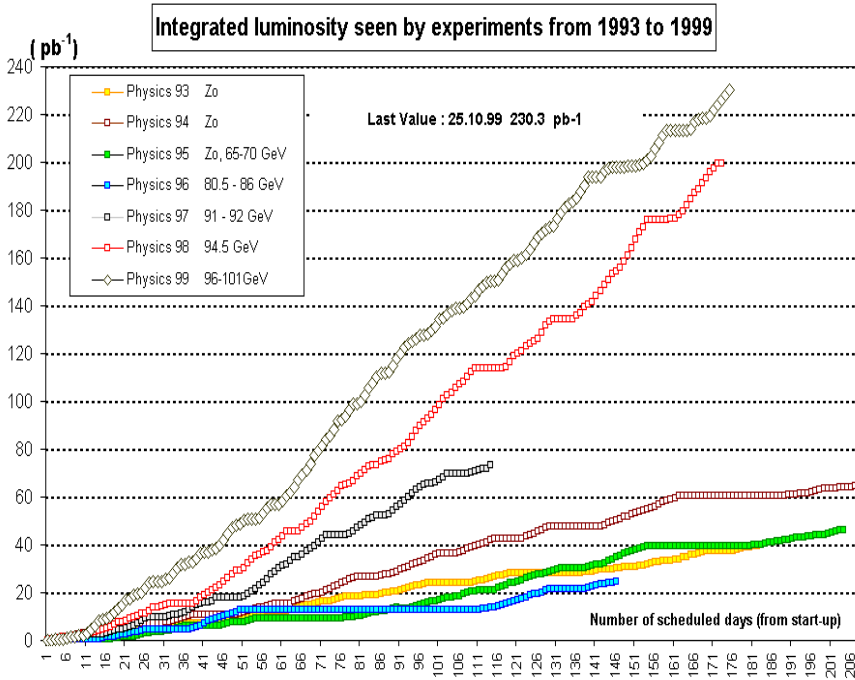


Fig. 1. Delivered integrated luminosity per LEP experiment

TABLE I

Data used for the combination of the Higgs boson searches from the four LEP experiments.

$\sqrt{s}$ (GeV)	Year	SM Higgs $\mathcal{L}$ ( $\text{pb}^{-1}$ )	MSSM Higgs $\mathcal{L}$ ( $\text{pb}^{-1}$ )	Charged Higgs $\mathcal{L}$ ( $\text{pb}^{-1}$ )
189	1998	683	683	690
192	1999	112	84	55
196	1999	265	185	132

The search for Higgs bosons is performed in different analysis channels with various signatures defined by the decay properties of the Higgs and  $Z$  bosons. The production and decay rates are mainly calculated in the framework of three theoretical models: the Standard Model with one Higgs doublet; the general two-doublet Higgs model where three neutral and two charged Higgs bosons are predicted; and the MSSM, where in addition, Higgs boson masses and couplings are related. In the MSSM one neutral Higgs boson is predicted to be light ( $m_h < 130$  GeV), while the charged Higgs bosons are heavier than the  $W$  boson.

## 2. Detectors

A typical LEP detector is shown in detail in Fig. 2. The particles produced at the interaction point in the center of the detector pass several subdetectors. All LEP detectors are equipped with micro-vertex detectors in order to measure tracks with precision near the interaction point. Following particles to larger radii, they pass a tracking system, electromagnetic calorimeters, hadron calorimeters and muon chambers. Figure 3 illustrates the principle of the particle identification. Detailed particle identification is also possible with the DELPHI RICH detector using Cherenkov light to determine particle masses.

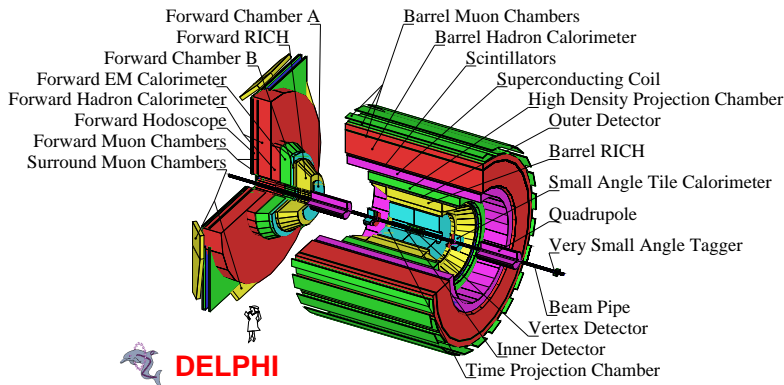


Fig. 2. A typical LEP detector

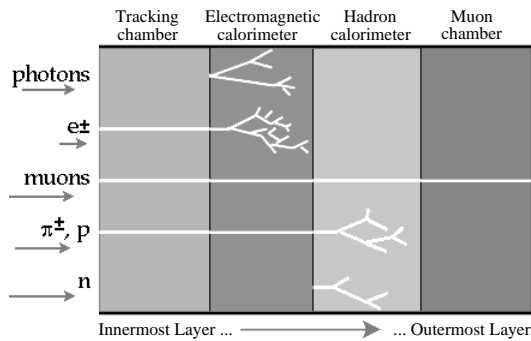


Fig. 3. Principle of particle identification

### 3. $ZZ$ background and Higgs boson candidates

The production cross sections for the background reactions are shown in Fig. 4. In 1998, the threshold of the  $ZZ$  production was passed and the  $ZZ$  production and decay became a dominant background for many searches. Thus, a good understanding of this background is very important to observe a signal. The good agreement of data and simulation is shown in Fig. 4 for the L3  $e^+e^- \rightarrow ZZ \rightarrow qq\ell\ell$  analysis [2]. An important method to reduce the  $ZZ$  background is based on the identification of  $b$ -quarks. As an example, the  $b$ -tagging performance from DELPHI is shown in Fig. 5.

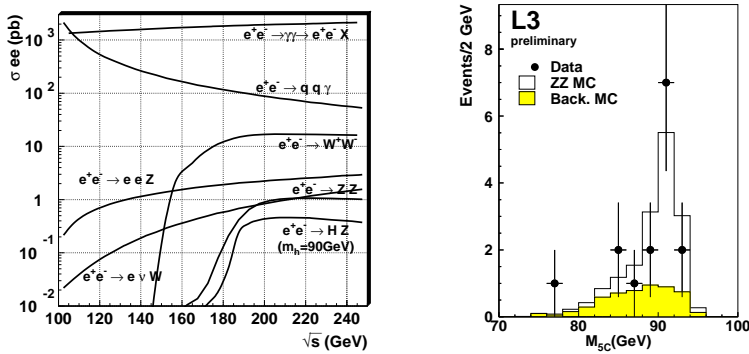


Fig. 4. Background production cross sections (left) and mass spectrum of  $ZZ$  events for data,  $ZZ$  and background simulation (right).

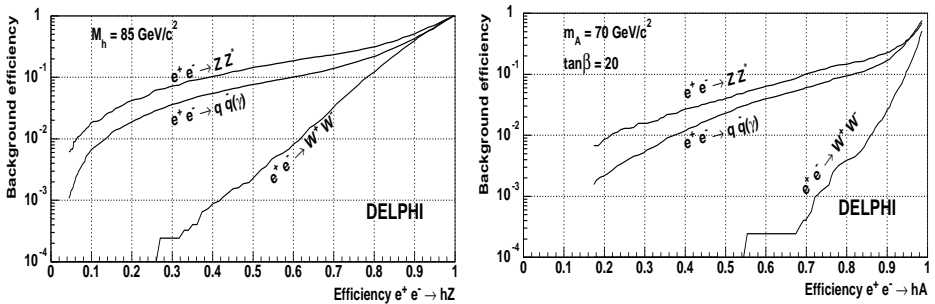


Fig. 5. Expected background as a function of efficiency for a simulated  $hZ$  and  $hA$  signal. The tagging of  $b$ -quarks reduces very strongly the  $WW$  process, where almost no  $b$ -quark decays are expected. Also,  $qq$  and  $ZZ$  processes are largely suppressed. While the Higgs bosons decay with more than about 85% branching ratio into  $b$ -quark pairs, the  $Z \rightarrow bb$  decay rate is only 15%.

Figures 6, 7 and 8 show examples of selected SM Higgs candidates which are compatible with  $ZZ$  background. The reconstructed invariant masses are 92.9 and 91.1 GeV in the four-jet event (Fig. 6). A typical jet-jet  $e^+e^-$  event signature is shown in Fig. 7 where the invariant masses are 85 and 96 GeV. One jet is  $b$ -tagged by a three dimensional reconstruction of a secondary vertex. In the jet-jet  $\mu^+\mu^-$  event (Fig. 8) the invariant mass of the muon pair is 92.3 GeV. The recoil mass of the muon pair is calculated for a better resolution of the hadron invariant mass, giving 93.4 GeV. All reconstructed masses are compatible with  $ZZ$  production, taking into account the errors on the measurements.

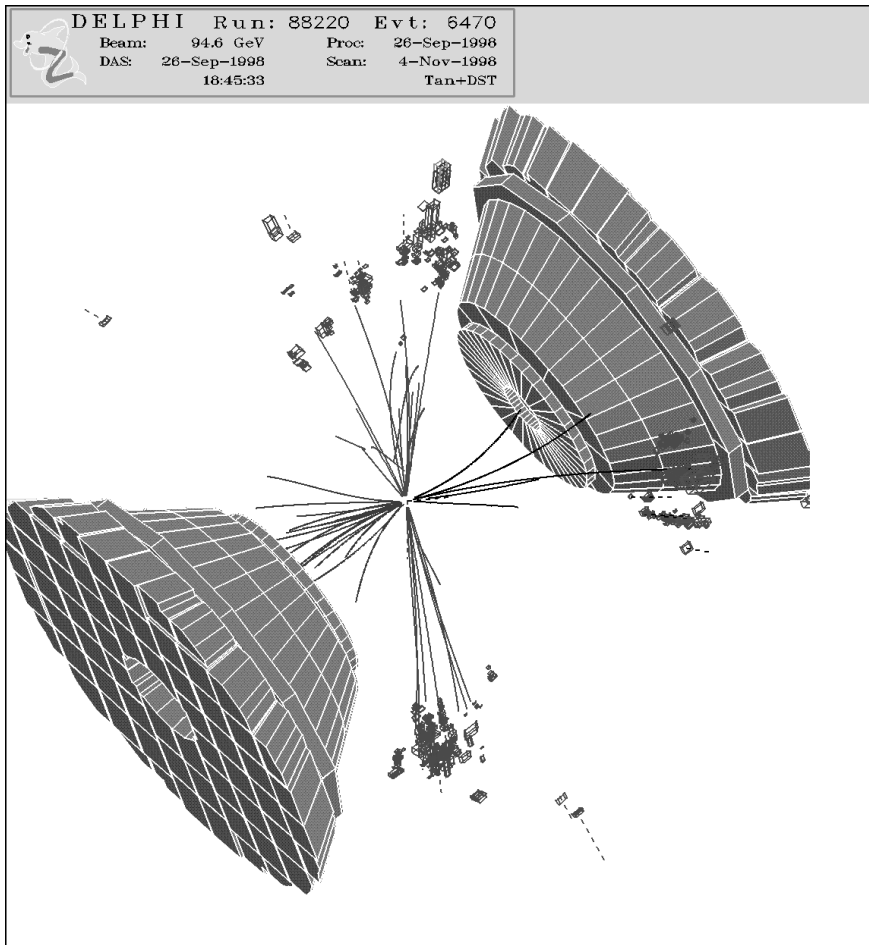


Fig. 6. DELPHI four-jet Higgs boson candidate event

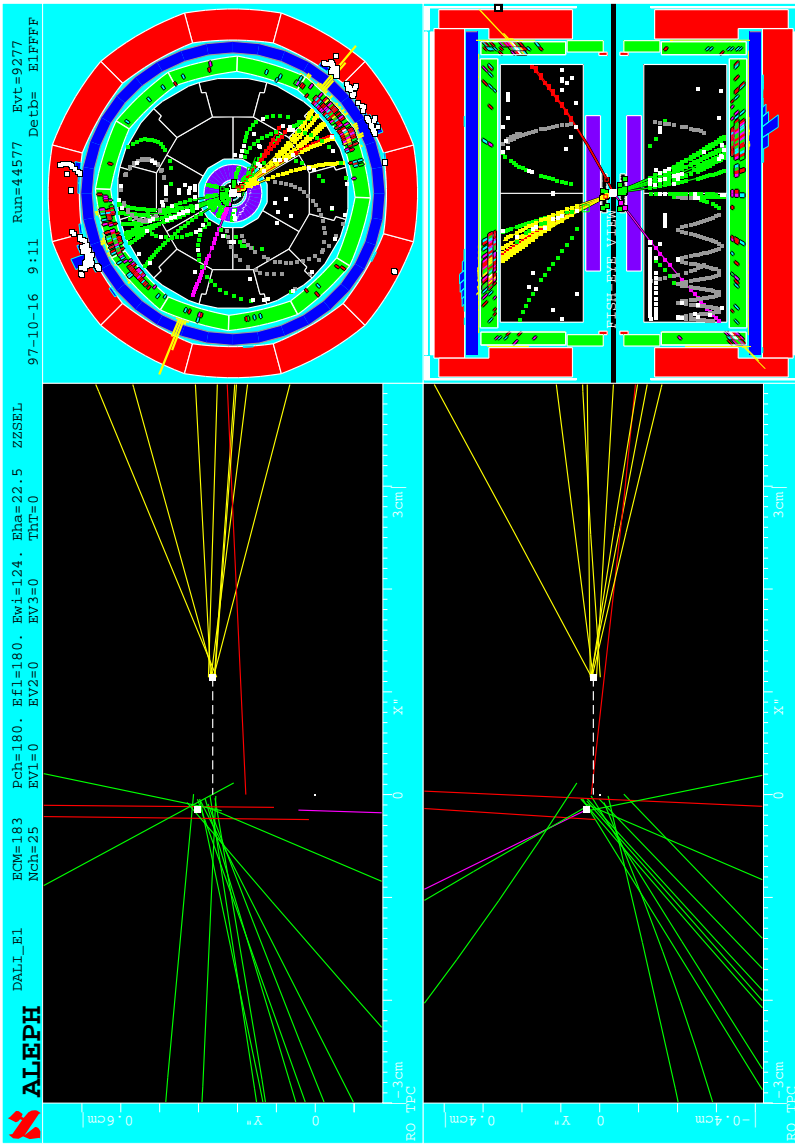


Fig. 7. ALEPH jet-jet  $e^+e^-$  Higgs boson candidate event. The upper right-hand figure shows nicely the separation of the  $e^+e^-$  pair from the two hadronic jets.

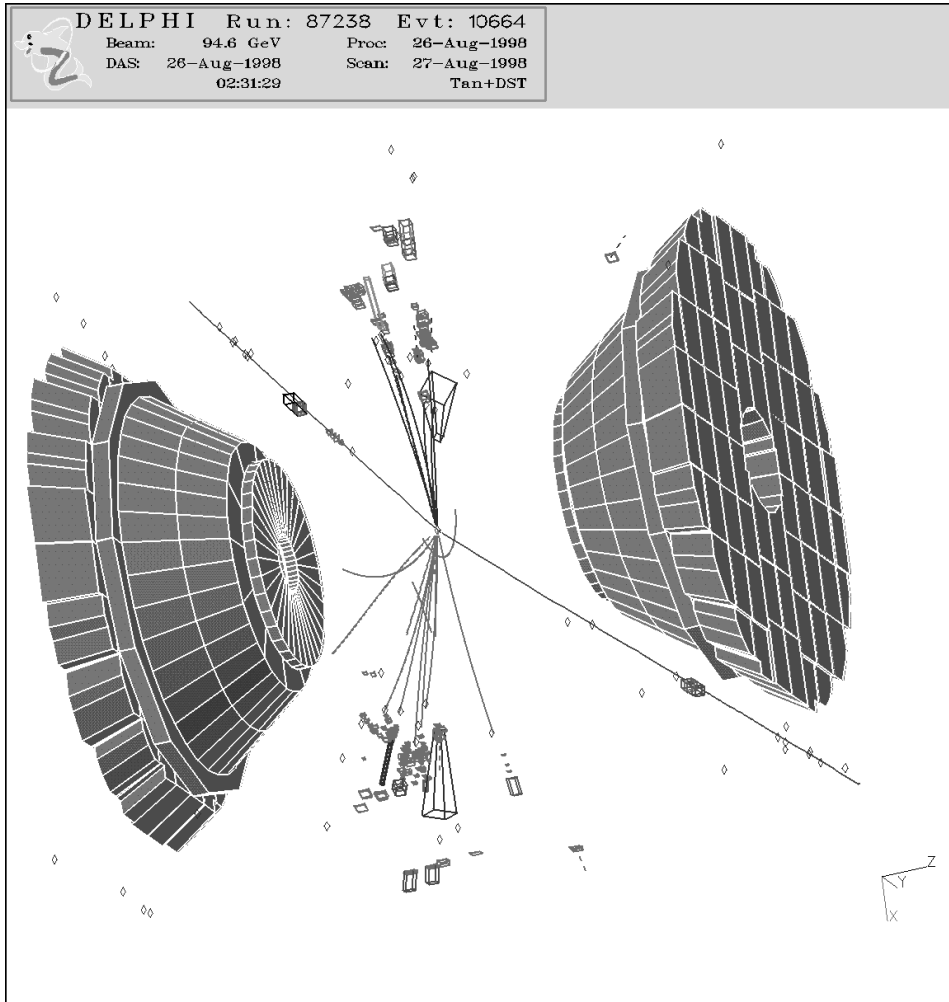


Fig. 8. DELPHI jet-jet  $\mu^+\mu^-$  Higgs boson candidate event

#### 4. Standard model Higgs boson

The search for the Standard Model Higgs boson is performed in the following decay channels:  $HZ \rightarrow bbqq$ ,  $bbee$ ,  $bb\mu\mu$ ,  $bb\tau\tau$  and  $bb\nu\nu$ . Figure 9 shows the number of data and background events as a function of the reconstructed Higgs boson mass. No indication of a signal is observed. A statistical analysis based on a likelihood function takes into account all search channels and gives the probability  $1 - CL_b$  that the data are compatible with the simulated background. Figure 10 shows this probability for 1998 data and including 1999 data up to 196 GeV center-of-mass energy. The limits on the SM Higgs boson mass derived from the probability  $CL_s$  that the expected signal and background is compatible with the data, and the corresponding  $\Delta\chi^2$  distribution are presented in Fig. 11.

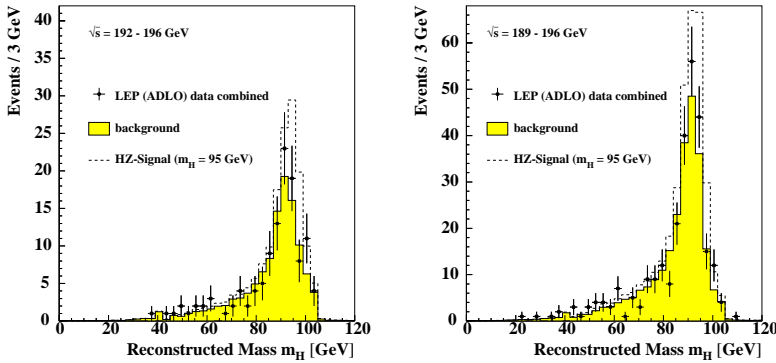


Fig. 9. Reconstructed mass distribution for combined data between 192 and 196 GeV (left) and including 189 GeV data (right).

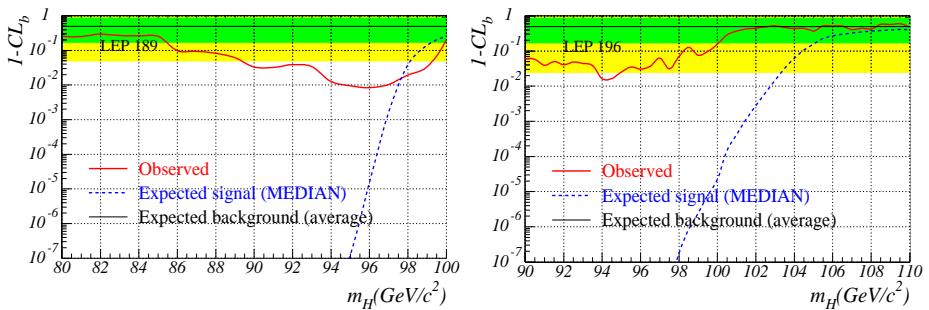


Fig. 10.  $1 - CL_b$  distribution for 1998 data (left) where a probability of 0.01 is observed for a 96 GeV Higgs boson. The data up to 196 GeV (right) reject the possibility of a 96 GeV Higgs boson. The grey areas show 1 and  $2\sigma$  regions.



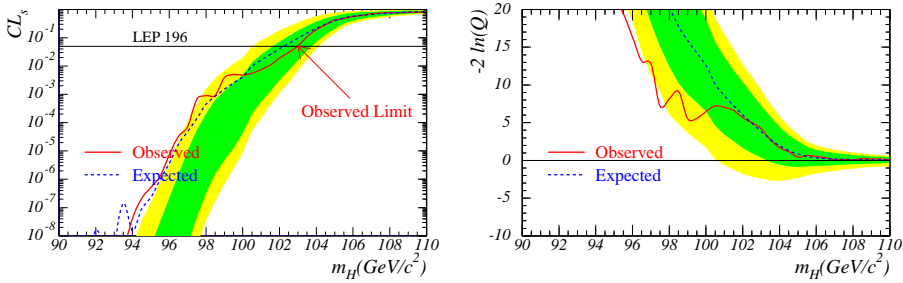


Fig. 11. Observed and expected SM Higgs boson mass limits, where 95% CL corresponds to  $CL_s = 0.05$  (left) and  $\Delta\chi^2$  values for a given Higgs boson mass (right). The grey areas show 1 and  $2\sigma$  regions.

The  $HZZ$  coupling is predicted to be smaller in many extensions of the SM. Figure 12 shows stringent limits on  $\xi^2$  from combined LEP data under the assumption that the Higgs boson decay modes do not change and the production rate is given by  $\sigma(HZ) = \sigma(H_{\text{SM}}Z) \cdot \xi^2$ .

An interesting extension of the SM is the addition of an extra Higgs singlet field. In this case two neutral massive Higgs bosons  $H$  and  $S$  are predicted, as is a massless, stable and non-interacting Majoron,  $J$ . The decays  $H \rightarrow JJ$  and  $S \rightarrow JJ$  lead to missing energy signatures. This process could be observed in the  $ZH$  and  $ZS$  production. The associated  $Z$  decay into a quark pair gives a signature of two jets and missing energy as in the  $H\nu\nu$  search channel. A limit from DELPHI on the mixing angle of  $H$  and  $S$  as a function of their masses is shown in Fig. 12.

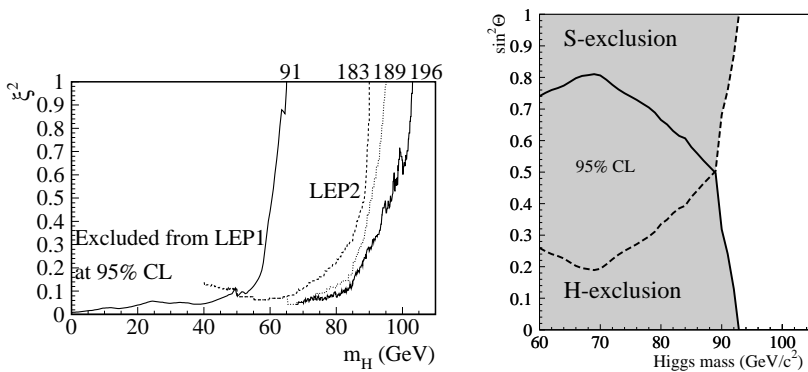


Fig. 12. Combined limit on the  $HZZ$  suppression factor  $\xi^2$  for LEP1 and LEP2 data up to 196 GeV center-of-mass energy (left) and DELPHI 189 GeV invisible Higgs limits in the plane of mass and mixing angle for  $H$  and  $S$  bosons (right).

## 5. MSSM Higgs bosons

The search for the scalar MSSM Higgs bosons is performed in the same search channels as for the SM Higgs boson. In addition, the pair-production process  $e^+e^- \rightarrow hA \rightarrow bbbb$  and  $\tau\tau bb$  is investigated, where  $h$  is the lighter scalar and  $A$  the pseudoscalar Higgs boson of the MSSM. Figure 13 shows the sum of the reconstructed Higgs boson masses. For simulated Higgs boson masses of 80 GeV, well below the kinematic production threshold, the inclusion of the data-taken in 1998 at 189 GeV increases significantly the discovery sensitivity.

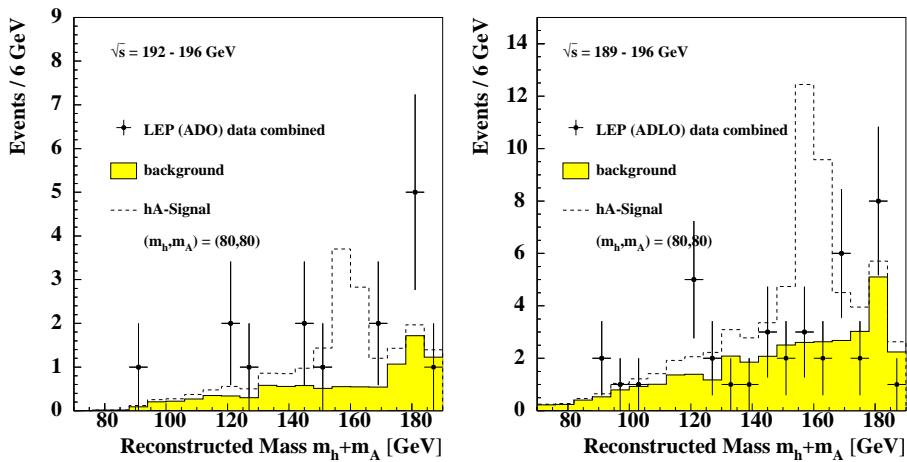
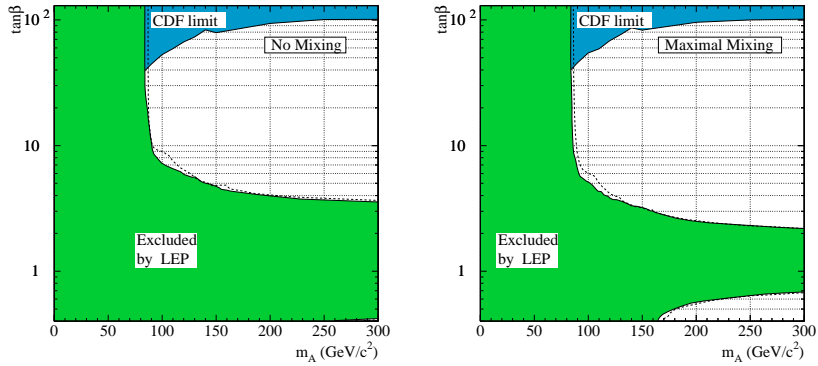
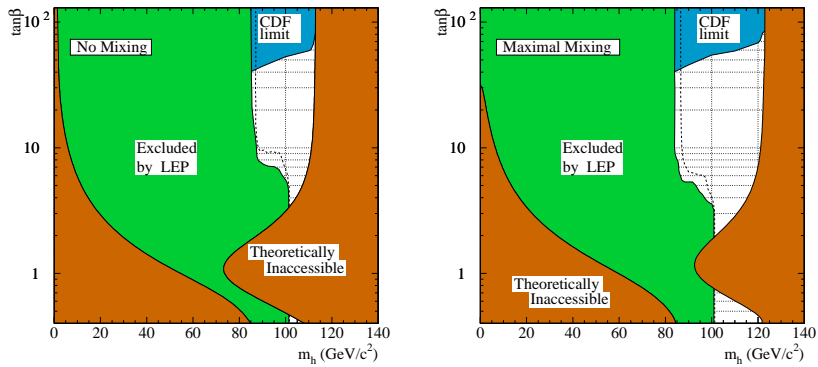
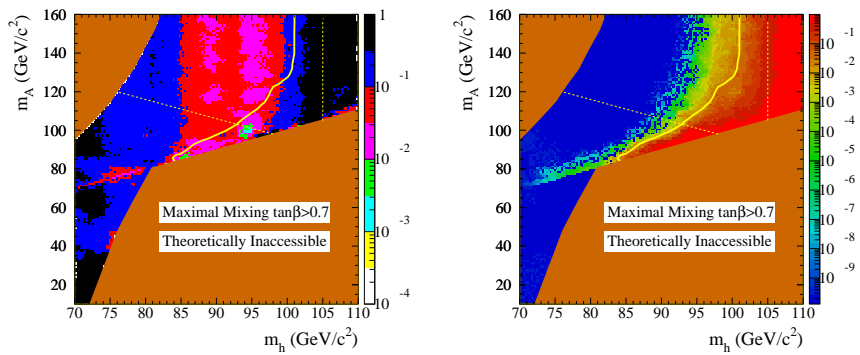


Fig. 13. Reconstructed mass distribution for combined data between 192 and 196 GeV (left) and including 189 GeV data (right).

Interpretations are given first for the so-called benchmark parameters, defined by a large Supersymmetric particle scale of 1 TeV and keeping all Supersymmetric parameters fixed. Figure 14 shows the excluded regions in the  $(m_A, \tan \beta)$  plane for no and maximal mixing in the scalar top sector, and Fig. 15 in the  $(m_h, \tan \beta)$  plane. The figures also show limits from the CDF experiment [3], based on the reaction  $bb \rightarrow bbbh$ , where the coupling is enhanced for large  $\tan \beta$ . Based on the benchmark parameters, details of the discovery ( $1 - CL_b$ ) and the exclusion ( $CL_s$ ) probabilities are shown in Fig. 16. The white lines give the 95% CL exclusion limit and the dashed lines the kinematic production limits for  $hA$  and  $hZ$  processes. No indication of a discovery is observed, where a  $5\sigma$  effect corresponds to  $1 - CL_b \approx 10^{-7}$  and the 95% CL corresponds to  $CL_s = 0.05$ .

Fig. 14. MSSM benchmark exclusion in the  $(m_A, \tan \beta)$  planeFig. 15. MSSM benchmark exclusion in the  $(m_h, \tan \beta)$  planeFig. 16. MSSM benchmark  $1 - CL_b$  (left) and  $CL_s$  (right) in the  $(m_h, m_A)$  plane

General parameter scans in the MSSM are very important in order to set reliable limits on  $h$  and  $A$  masses. For LEP1 newly unexcluded mass regions were pointed out [4], and for 172 GeV LEP2 data stringent mass limits disappeared completely [5] allowing a Higgs boson to escape detection although it could have been kinematically produced. The latest general scan results with 189 GeV DELPHI data are shown in Fig. 17 [6]. The corresponding parameter ranges are listed in Table II. The limit on the  $h$  mass is at 75 GeV compared to 82 GeV for the DELPHI benchmark result [7]. The  $h$  and  $A$  mass limits are given by the light grey edge intruding the LEP2 excluded area. An extension of the  $A$  range to  $\pm 2$  does not change the mass limit, but it increases the maximal Higgs mass to 130 GeV. Reduced mass limits are also presented by OPAL [8].

In addition to the scanning over the Supersymmetric parameters, more precise mass, cross section and branching ratio calculation based on 2-loop Full-Diagrammatic Calculations (FDC) [9] are used. Figure 17 shows also that the maximal  $h$  mass is reduced by about 10 GeV and the maximum is already reached for smaller mixing values in the scalar top sector. The reduction of the maximal Higgs boson mass is important for LEP physics, since it affects the excluded  $\tan \beta$  range (see Fig. 15) and reduces the uncovered parameter region. LEP comes closer to a definitive test of the MSSM.

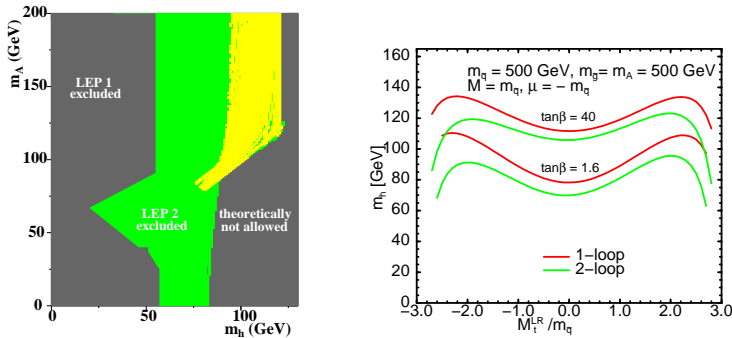


Fig. 17. DELPHI general scan leading to reduced mass limits compared to the benchmark results (left), and comparison of 1- and 2-loop FDC as a function of the mixing  $A$  in the scalar top sector (right).

TABLE II

General scan parameter ranges				
Parameter	$m_{sq}$ (GeV)	$m_g$ (GeV)	$\mu$ (GeV)	$A$
Range	200—1000	200—1000	−500—500	−1—+1

## 6. Charged Higgs bosons

New calculations of the production cross section  $e^+e^- \rightarrow H^+H^-$  include 1-loop radiative corrections [10]. The cross section for  $\sqrt{s} = 190$  GeV is shown in Fig. 18. Compared to the tree-level calculations, the cross section is about 7.5% larger for  $2 < \tan \beta < 15$  independent of the charged Higgs boson mass. Note that a 15% reduction is obtained for very small and very large  $\tan \beta$  values. The results from the LEP experiments are still based on tree-level calculations. Figure 19 shows the reconstructed  $H^\pm$  mass for data, simulated signal and background. Mass limits based on a statistical analysis are also shown in Fig. 19. The sensitivity in the leptonic search channel is larger, since the irreducible  $WW$  background leads only in 1% of cases to the  $\tau\nu\tau\nu$  final state. Independent of the charged Higgs boson branching fraction, a mass limit of 77 GeV is set at 95% CL.

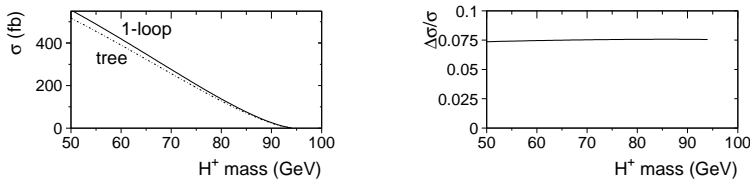


Fig. 18.  $e^+e^- \rightarrow H^+H^-$  cross section including 1-loop radiative corrections

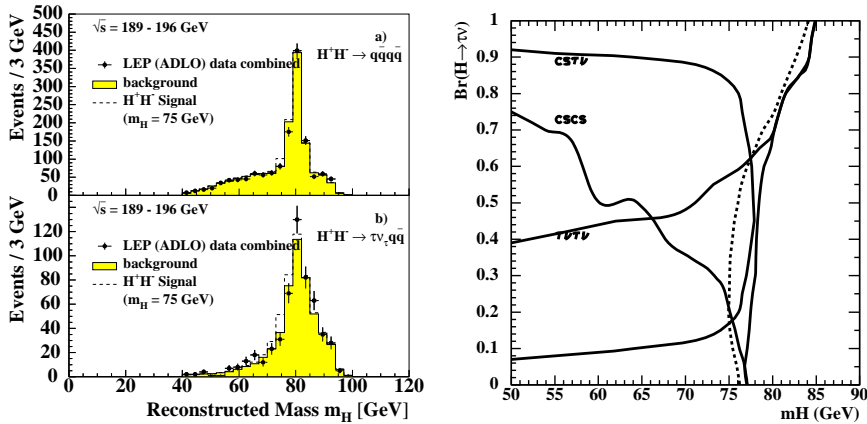


Fig. 19. Reconstructed  $H^\pm$  mass in the hadronic and semi-leptonic search channels (left), and resulting mass limits (right) including the leptonic channel and the combination of all three channels. In addition, the expected mass limit is shown.

## 7. Supersymmetric particles

The clean environment of the LEP  $e^+e^-$  collider and the good hermiticity of the LEP detectors allow detailed searches for Supersymmetric particles. Since the lightest Supersymmetric particle is expected to be neutral and stable, it escapes detection, leading to a missing energy signature. A typical candidate event taken at 200 GeV center-of-mass energy with the DELPHI detector is shown in Fig. 20. The event shows two acoplanar jets indicating that energy, possibly from neutralinos, has escaped detection. A variety of searches for events with leptons, quarks, and missing energy is performed. No indication of Supersymmetry has been found yet. Many mass limits close to the kinematic production threshold are set with 189 GeV data [11].

A few examples of data and background comparisons for the data-taking up to 196 GeV are presented. The number of observed and expected events

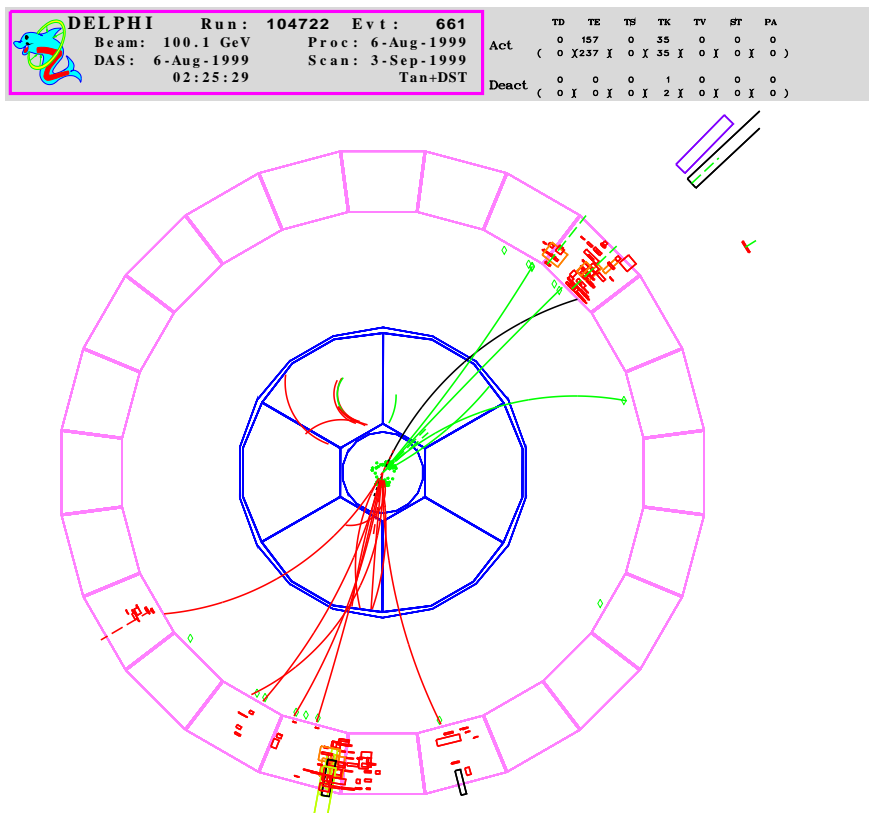


Fig. 20. DELPHI candidate event  $e^+e^- \rightarrow \chi_1^0 \chi_2^0 \rightarrow \chi_1^0 \chi_1^0 qq$ , compatible with background for example from  $ZZ \rightarrow qq\nu\nu$  production.

in the search for sleptons is shown in Fig. 21 as a function of slepton and neutralino masses. The large value of the top mass could imply a large mixing for scalar top quarks, thus rendering the lighter scalar top to be the lightest Supersymmetric quark. A comparison of data and simulated background events in the search for scalar top and scalar bottom quarks is given in Fig. 22. The number of data events is compatible with the simulated background expectation. The decay  $\chi_2^0 \rightarrow \chi_1^0 \gamma$  is also possible. A signal could be observed in the single or double photon spectra. Figure 23 shows no indication of deviation between data and background simulation.

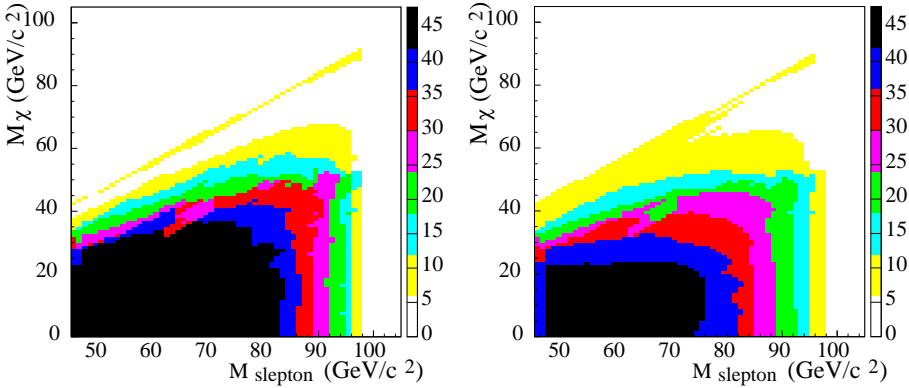


Fig. 21. Comparison of the number of data (left) and simulated background (right) events in the slepton search.

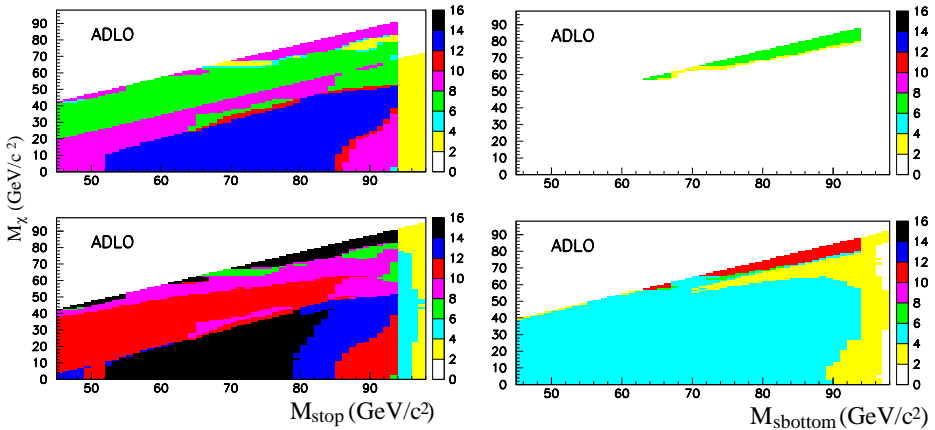


Fig. 22. Comparison of the number of data (upper) and simulated background (lower) events in the stop (left) and sbottom (right) search.

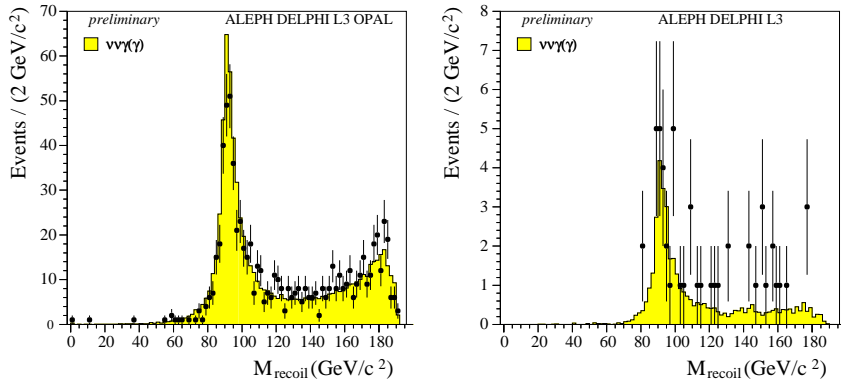


Fig. 23. Recoil mass spectra of single (left) and double (right) photon production

## 8. Conclusions

No indication of new particles is observed. The combination of the data from the four LEP experiments provides significantly more detection sensitivity. The SM Higgs mass is larger than 102.6 GeV at 95% CL. In the remaining year of LEP operation, the SM Higgs boson could be discovered up to 110 GeV at  $5\sigma$  or excluded up to about 114 GeV at 95% CL. Stringent mass limits are set in general extensions of the SM, even for strongly reduced  $HZ$  production rates. The charged Higgs boson mass is larger than 77 GeV which is close to the  $W$  mass, where  $WW$  production gives a large irreducible background. Large regions of the MSSM parameter space are excluded, in particular, small  $\tan\beta$  values. In future studies, the model-independent presentations of the experimental results should be even more emphasized and general parameter scans should be favored over benchmark interpretations.

## REFERENCES

- [1] The Four LEP Experiments and the Higgs and SUSY LEP Working Groups, LEPC presentations, CERN, 7 Sep. 1999.
- [2] L3 Coll., EPS Tampere 1999, contributed paper 6-249.
- [3] CDF Coll., EPS Tampere 1999, talk by J.Valls, to be published in the proceedings.
- [4] J. Rosiek, A. Sopczak, *Phys. Lett.* **B341**, 419 (1995).
- [5] A. Sopczak, *Eur. Phys. J.* **C7**, 107 (1999).
- [6] DELPHI Coll., EPS Tampere 1999, contributed paper 7-117.



- [7] DELPHI Coll., EPS Tampere 1999, contributed paper 6-231.
- [8] OPAL Coll., CERN-EP/99-096, submitted to *Eur. Phys. J.*
- [9] S. Heinemeyer, W. Hollik, G. Weiglein, *Eur. Phys. J.* **C9**, 343 (1999).
- [10] A. Kraft, PhD Thesis, Karlsruhe 1999, and private communications.
- [11] The Four LEP Experiments and the SUSY LEP Working Group, EPS Tampere 1999, contributed paper 7-716.